



Universiteit  
Leiden  
The Netherlands

## **Transdermal iontophoresis of dopaminergic (pro) drugs : from formulation to in vivo application**

Ackaert, O.

### **Citation**

Ackaert, O. (2010, April 28). *Transdermal iontophoresis of dopaminergic (pro) drugs : from formulation to in vivo application*. Retrieved from <https://hdl.handle.net/1887/15336>

Version: Corrected Publisher's Version

License: [Licence agreement concerning inclusion of doctoral thesis in the Institutional Repository of the University of Leiden](#)

Downloaded from: <https://hdl.handle.net/1887/15336>

**Note:** To cite this publication please use the final published version (if applicable).

# 7

## **The *in vitro* and *in vivo* evaluation of new synthesized prodrugs of 5-OH-DPAT for iontophoretic delivery**

Oliver W. Ackaert<sup>a\*</sup>, Jeroen De Graan<sup>c\*</sup>, Romano Capancioni<sup>a</sup>, Oscar E. Della Pasqua<sup>b,e</sup>, Durk Dijkstra<sup>c</sup>, Ben H. Westerink<sup>d</sup>, Meindert Danhof<sup>b</sup> and Joke A. Bouwstra<sup>a</sup>

<sup>a</sup>Division of Drug Delivery Technology, Leiden/Amsterdam Center for Drug Research, Leiden, The Netherlands

<sup>b</sup>Division of Pharmacology, Leiden/Amsterdam Center for Drug Research, Leiden, The Netherlands

<sup>c</sup>Department of Medicinal Chemistry, University Center of Pharmacy, University of Groningen, Groningen, the Netherlands

<sup>d</sup>Department of biomonitoring and sensing, University Center of Pharmacy, University of Groningen, Groningen, The Netherlands

<sup>e</sup>Clinical Pharmacology and Discovery Medicine, GlaxoSmithKline, Greenford, United Kingdom

\* Contributed equally as first author

adapted from *Journal of controlled release*. 2010. *in press*.

## Abstract

The feasibility of transdermal iontophoretic transport of 4 novel ester prodrugs of 5-OH-DPAT (glycine-, proline-, valine- and  $\beta$ -alanine-5-OH-DPAT) was investigated *in vitro* and *in vivo*. Based on the chemical stability of the prodrugs, the best candidates were selected for *in vitro* transport studies across human skin. The pharmacokinetics and pharmacodynamic effect of the prodrug with highest transport efficiency, was investigated in a rat model. The *in vitro* transport, plasma profile and pharmacological response were analyzed with compartmental modeling. Valine- and  $\beta$ -alanine-5-OH-DPAT were acceptably stable in the donor phase and showed a 4-fold and 14-fold increase in solubility compared to 5-OH-DPAT. Compared to 5-OH-DPAT, valine- and  $\beta$ -alanine-5-OH-DPAT were transported less and more efficiently across human skin, respectively. Despite a higher *in vitro* transport, lower plasma concentrations were observed following 1.5 h current application ( $250 \mu\text{A}\cdot\text{cm}^{-2}$ ) of  $\beta$ -alanine-(S)-5-OH-DPAT in comparison to (S)-5-OH-DPAT. However the prodrug showed higher plasma concentrations post-iontophoresis, explained by a delayed release due to hydrolysis and skin depot formation. This resulted in a pharmacological effect with the same maximum as 5-OH-DPAT, but the effect lasted for a longer time. The current findings suggest that  $\beta$ -alanine-5-OH-DPAT is a promising prodrug, with a good balance between stability, transport efficiency and enzymatic conversion.

**Keywords:** prodrugs, stability, iontophoresis, PK-PD

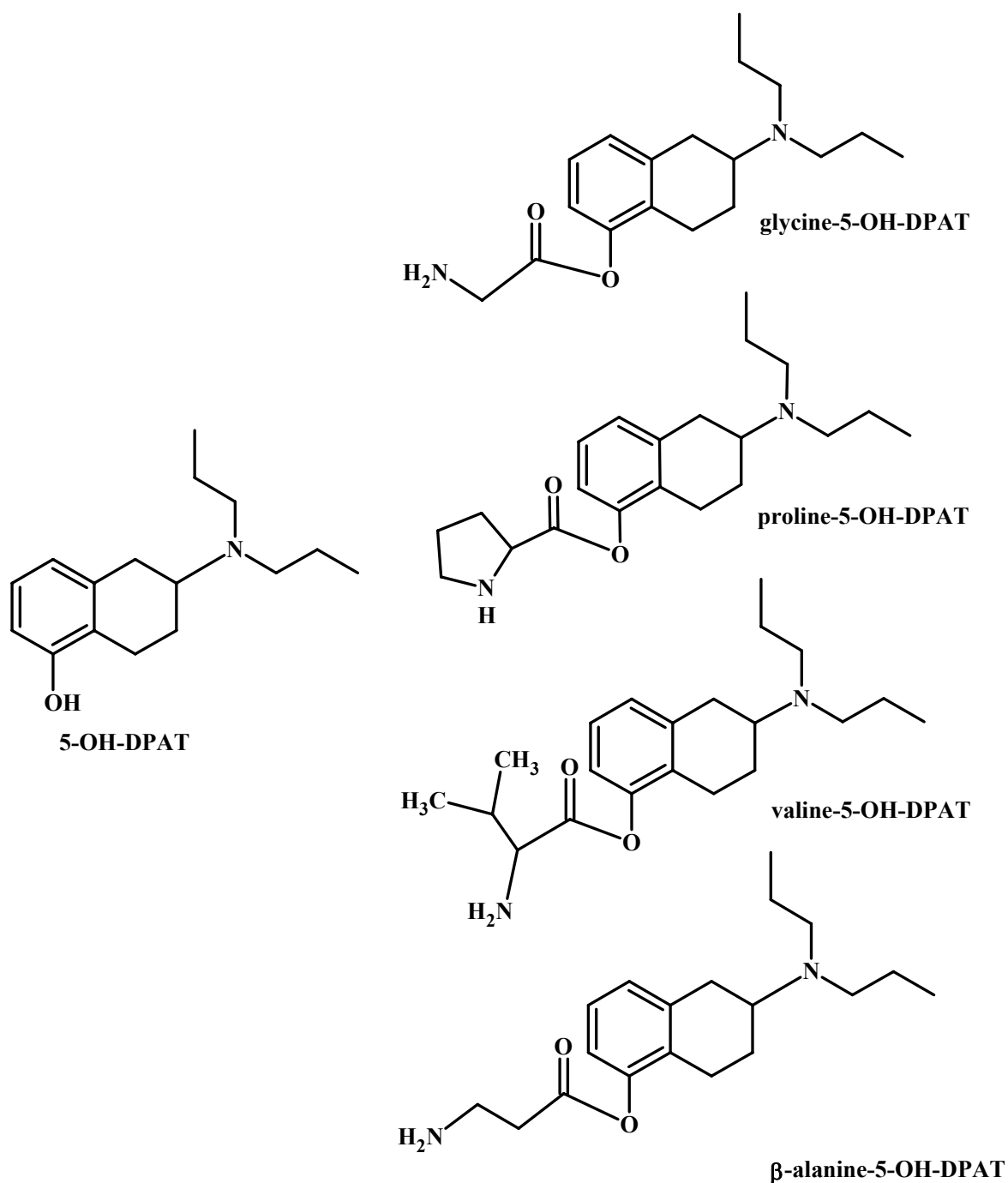


**Figure 1:** Molecular structure of 5-OH-DPAT and the 4 synthesized prodrugs, glycine-5-OH-DPAT, proline-5-OH-DPAT, valine-5-OH-DPAT and  $\beta$ -alanine-5-OH-DPAT

## 1 Introduction

Transdermal delivery has been explored thoroughly as an alternative for oral delivery and injections. However, the main hurdle for transdermal delivery is the barrier function of the skin located in the outermost layer of the skin, the stratum corneum. An attractive approach to overcome this main barrier for drug delivery is iontophoresis. By applying a small current across the skin it is possible to enhance the transport of low molecular weight molecules across the skin. One of the interesting properties of this technique is the possibility to modulate the transport rate into and through the skin. This is an important advantage for drugs with a narrow therapeutic window, such as dopamine agonists (e.g. rotigotine, apomorphine, pergolide, 5-OH-DPAT). Most of the dopamine agonists are considered moderate lipophilic and have a relative low solubility in aqueous solutions [2-4]. For this reason, besides a low efficiency in iontophoretic transport, the low solubility of dopamine agonists can be a limitation for application with transdermal iontophoresis. Increasing the maximum solubility in the donor phase can be achieved by adjusting the donor phase (co-solvent, surfactant, source of Cl<sup>-</sup> ions) or by changing the salt form. Another approach is the use of prodrugs with the desired physicochemical properties to overcome the problem of solubility and increase the efficiency in iontophoretic transport [5]. The principle goal of synthesizing prodrugs is to chemically modify an existing pharmacologically active drug in a form that can be reversed to the parent drug *in vivo*, with the aim to change the physicochemical and/or pharmacokinetic properties. Moreover for transdermal delivery a prodrug should be enzymatically metabolized in a controllable and predictable manner once it has penetrated the main barrier, the stratum corneum [6-8].

The main focus of the present study is to identify a prodrug that is transported efficiently with transdermal iontophoresis and is hydrolyzed during transport through the skin. This implies a good balance between the transport rate and the rate of enzymatic conversion of the prodrug. Previous studies showed that transdermal iontophoretic delivery of 5-OH-DPAT resulted in a strong pharmacological response, which is believed to meet the requirements for symptomatic therapy with a reasonable patch size and acceptable current density [1, 9]. However further improving the iontophoretic delivery could merely enhance the clinical applicability of this potent dopamine agonist by reduction of the patch size and more importantly minimization of the current density. Therefore 5-OH-DPAT, a dopamine agonist with limited aqueous solubility, was esterified with 4 different natural occurring amino acids (Figure 1). These amino acids contain an extra chargeable aminogroup, providing the possibility to investigate the influence of an additional charge on the

iontophoretic delivery of 5-OH-DPAT. The stability of these 4 prodrugs is investigated and the most stable compounds are selected for transdermal iontophoretic transport. Depending on the iontophoretic transport efficiency of the selected prodrugs *in vitro* across human stratum corneum and dermatomed human skin, the *in vivo* transport of the most promising candidate is further investigated. The plasma profile and the pharmacodynamic effect are monitored simultaneously in an animal model under anaesthetized conditions. Both *in vitro* and *in vivo* transport profiles are analyzed using compartmental modeling. Taking the hydrolysis of the prodrug into account, an adaptation to existing kinetic models is made to describe the transdermal iontophoretic delivery *in vivo* [1, 9].

## 2 Materials and Methods

### 2.1 General synthesis of the glycine, L-proline, $\beta$ -alanine and L-valine esters of 5-OH-DPAT

The full description of the synthesis of the 4 prodrugs of 5-OH-DPAT is described elsewhere [10]. Briefly, 5-OH-DPAT was esterified to the N-protected amino acid with the carbodiimide coupling reagent N-(3-dimethylaminopropyl)-N'-ethylcarbodiimide (EDC). 1-Hydroxybenzotriazole (HOBt) was added to suppress racemisation. The deprotection of the Boc-protected compound was carried out in 4N HCl in dioxane. After removal of the solvent and evaporation *in vacuo*, the solid hygroscopic foams were reprecipitated from dry methanol with dry ether to remove excess dioxane. The prodrugs were obtained as white hygroscopic dihydrochloride salts with a purity of >95% (HPLC).

### 2.2 Materials

5-OH-DPAT and 5-hydroxy-2-(N-n-propyl-N- $\alpha,\alpha$ -dideutero-propylamino)-tetralin ( $d_2$ -5-OH-DPAT) (HBr salts, purity >98%) were synthesized at the Department of Medicinal Chemistry of the University of Groningen, Groningen, the Netherlands. Silver, silver chloride (purity >99.99%), trypsin (Type III from bovine pancreas) and trypsin inhibitor (Type II-S from soybean) were obtained from Sigma-Aldrich (Zwijndrecht, The Netherlands). Acetaminophen was purchased from Brocacef BV (Maarsse, the Netherlands) and D-Mannitol was obtained from BDH Laboratory supplies (Poole, UK). Spectra/Por<sup>®</sup> RC dialysis membrane disks (cut off value of 6000-8000 Da) were purchased from Spectrum laboratories, Inc (Rancho Dominguez, Ca, USA). Tetrahydrofuran (THF, stabilized, purity >99.8%) was obtained from Biosolve (Valkenswaard, the Netherlands). Triethylamine (TEA,

purity >99%) was obtained from Acros Organics (Geel, Belgium). All other chemicals and solvents were of analytical grade. All solutions were prepared in Millipore water with a resistance of more than 18 M $\Omega$ .cm.

### 2.3 Stability of glycine-, proline-, valine- and $\beta$ -alanine-5-OH-DPAT

The stability of the prodrugs was investigated under various conditions. At the starting point 1 mg.ml<sup>-1</sup> of proline- and glycine-5-OH-DPAT and 0.02 mg.ml<sup>-1</sup> of valine- and  $\beta$ -alanine-5-OH-DPAT were dissolved in the buffer solution. The buffer solution was citric buffer (5 mM, pH 5.0 + 4 g.L<sup>-1</sup> NaCl + 23.1 g.L<sup>-1</sup> D-mannitol), PBS pH 6.2 (NaCl: 8 g.l<sup>-1</sup>, KCl: 0.19 g.l<sup>-1</sup>, Na<sub>2</sub>HPO<sub>4</sub>.2H<sub>2</sub>O: 0.43 g.l<sup>-1</sup>, KH<sub>2</sub>PO<sub>4</sub>: 0.97 g.l<sup>-1</sup>) or PBS pH 7.4 (NaCl: 8 g.l<sup>-1</sup>, Na<sub>2</sub>HPO<sub>4</sub>: 2.86 g.l<sup>-1</sup>, KH<sub>2</sub>PO<sub>4</sub>: 0.2 g.l<sup>-1</sup>, KCl: 0.19 g.l<sup>-1</sup>). The solutions were continuously stirred and kept constant at the desired temperature, using a thermostat controlled water bath. If required a circular sheet of human stratum corneum (HSC) ( $\phi$ =18 mm) was added to the solution and a current of 320  $\mu$ A was applied. At regular time intervals samples were taken from the solution and diluted in Millipore water, containing 0.1% trifluoroacetic acid [11] to stop degradation. Both the amount of remaining prodrug and the parent drug 5-OH-DPAT were quantified by RP-HPLC. The amount of remaining prodrug was plotted as a function of time to calculate the first order rate constant of hydrolysis and the corresponding half life.

### 2.4 Maximum solubility of valine-5-OH-DPAT and $\beta$ -alanine-5-OH-DPAT

The solubility studies of the different compounds were carried out as described elsewhere [3]. Briefly, each compound was solubilized in citric buffer 5 mM, pH 5.0 + 4 g.L<sup>-1</sup> NaCl + 23.1 g.L<sup>-1</sup> D-mannitol. Subsequently the pH in each test tube was adjusted to pH 5.0 with 1M NaOH or 1M HCl under continuous shaking. Each solution was shaken for 48h, after which the solution was centrifuged and filtered. The concentration in each solution was determined with HPLC. Due to the limited availability of the compound and the relative high solubility, this assay was performed in monoplicate (n=1).

### 2.5 *In vitro* transport studies

The preparation of dermatomed human skin (DHS) and human stratum corneum was performed according to the method described previously [12]. All transport experiments were carried out as described elsewhere [12]. The donor formulation (citric buffer 5 mM, pH 5.0, NaCl: 4 g.L<sup>-1</sup>, D-mannitol: 23.1 g.L<sup>-1</sup>), containing the solute, was added to the anodal chamber. The cathodal chamber was filled with PBS

pH 7.4. Unless described differently, the acceptor phase, maintained at 32°C, was continuously perfused with PBS 7.4 at a flow rate of 7.0 ml.h<sup>-1</sup>. The following protocol was used: 6h passive diffusion + 9h iontophoresis (500 μA.cm<sup>2</sup>) + 5h passive diffusion. Samples were collected every hour with an automatic fraction collector (ISCO Retriever IV, Beun De Ronde BV, Abcoude, The Netherlands). To stop the hydrolysis after transport through the skin and before analysis TFA (0.1% v/v) was added to each sample. The specific conditions of the individual transport studies are described below.

#### 2.5.1 Iontophoretic delivery of valine-OH-DPAT and β-alanine-5-OH-DPAT

The iontophoretic delivery of valine-5-OH-DPAT across HSC and DHS was studied at a concentration of 3.9 mM.

Iontophoretic delivery of β-alanine-5-OH-DPAT across HSC was studied at 3 different concentrations (1.5 mM, 3.9 mM or 7.0 mM). For the transport study with 1.5 mM as donor phase the current was only applied for 7h, after which the experiment was stopped. Transport studies across DHS were performed with a donor concentration of 3.9 mM. For all experiments PBS pH 7.4 was used as acceptor phase.

#### 2.5.2 Electroosmotic flux across HSC

The electroosmotic flux across HSC was investigated during iontophoretic transport of valine- and β-alanine-5-OH-DPAT (3.9 mM), buffered at pH 5.0. Acetaminophen (15 mM) was added to the donor phase as a marker for the electroosmosis. PBS pH 7.4 was used as acceptor phase.

#### 2.6 Hydrolysis during transport across HSC and DHS

The prodrugs valine-5-OH-DPAT and β-alanine-5-OH-DPAT are expected to hydrolyze during transdermal transport. Although stratum corneum is considered as the main barrier of the skin, the majority of the enzymes, such as esterases can be found in the epidermis [13]. Therefore the hydrolysis of the prodrugs (donor conc: 3.9 mM) was determined during iontophoresis across HSC and DHS. In case of valine-5-OH-DPAT, PBS pH 6.2 was used as acceptor phase and for β-alanine-5-OH-DPAT PBS pH 7.4 was used. The remaining prodrug was determined in the acceptor phase every hour after transport, taking the degradation in the donor phase and acceptor phase into account.

### 2.7 PK-PD studies

In the following studies the pharmacokinetic (PK) and pharmacodynamic (PD) properties of  $\beta$ -ala-(S)-5-OH-DPAT following transdermal iontophoretic delivery were determined simultaneously by taking blood samples (PK) and using on-line microdialysis (PD). For these studies, the active enantiomer (S)-5-OH-DPAT, was esterified with  $\beta$ -alanine. Animal procedures were conducted in accordance with guidelines published in the NIH guide for the care and use of laboratory animals and all protocols were approved by the Institutional Animal Care and Use Committee of the University of Groningen. The surgical, experimental and analytical procedures were identical to the methods used for PK-PD studies performed with the parent drug (S)-5-OH-DPAT [1]. A brief description is outlined below.

#### 2.7.1 Animals

The pharmacokinetic-pharmacodynamic (PK-PD) studies were performed in albino male wistar rats (280-340 g) obtained from Harlan (Horst, the Netherlands). Prior to surgery the animals were housed at least 1 week in plexiglas cages, maximum 6 animals per cage with free access to water and standard laboratory chow. The cages were placed in a room with a controlled temperature at 21 °C and controlled humidity between 60-65% and a light-dark cycle of 12h.

#### 2.7.2 Surgical procedures

Prior to surgery the rats were anaesthetized with Isofluran 2% in N<sub>2</sub>O/O<sub>2</sub> (2/1). The permanent cannulations in the femoral vein and femoral artery were performed using silicone catheters (inner diameter (I.D.): 0.5 mm; outer diameter (O.D.): 0.9 mm) (UNO BV, Zevenaar, The Netherlands). After the cannulation the rats were kept under anaesthetized condition and mounted into a stereotaxic frame for the implementation of the microdialysis probes. A Y-shaped dialysis probe was used for the experiments, with an exposed tip length of 3 mm. The dialysis cannula (I.D.: 0.24 mm; O.D.: 0.34 mm) was prepared from polyacrylonitrile/sodium methallyl sulfonate copolymer (AN 69, Hospal, Bologna, Italy). The microdialysis cannula was implanted in the striatum. The following coordinates were used according to the atlas of Paxinos and Watson [14]: AP +0.9, LM  $\pm$  3.0 relative to bregma, and Vd – 6.0 below dura. The dialysis probe, filled with Ringer solution (140 mM NaCl, 3.0 mM KCl, 1.2 mM CaCl<sub>2</sub>, 1.0 mM MgCl<sub>2</sub>), was positioned and fixed in the burr hole under stereotaxic guidance. Thereafter the rats were housed solitary.

### 2.7.3 Experimental procedures

The PK-PD studies were performed 15-20 h after permanent cannulation and implementation of the probes. The rats were anaesthetized prior to and kept under anesthetized condition during the experiment with Hypnorm<sup>®</sup> and Dormicum<sup>®</sup> at a starting dose of 0.5 mL.kg<sup>-1</sup> and subsequent 1h doses of 0.17 mL.kg<sup>-1</sup>.

The donor solution consisted of  $\beta$ -ala- (S)-5-OH-DPAT (3.9 mM), buffered in citric buffer 5 mM at pH 5.0. Before the start of the experiment, the hair of the back of the anesthetized rat was removed with an electrical clipper and scalpel. 15 min after attaching the patches to the skin surface, the cathodal patch was filled with PBS pH 7.4 and the anodal patch was filled with donor solution. The volume of the patches was 2.3 ml and the active area was 2.5 cm<sup>2</sup>. The protocol for the transdermal iontophoretic PK-PD studies was: 15 min passive diffusion + 90 min current application (250  $\mu$ A.cm<sup>-2</sup>). The patch was removed and the skin was wiped using tissue paper. Blood samples were taken at regular time intervals: 0, 15, 30, 45, 60, 75, 90, 105, 120, 135, 165, 195, 225, 255, 285 min. The blood samples (0.2 ml) were collected using lithium-heparin containing tubes (Microvette<sup>®</sup> 200 Plasma/Lithium Heparin, Sarsted BV, Etten-Leur, the Netherlands) and subsequently the plasma samples were separated from the blood cells by centrifugation. The samples were kept at -20 °C prior to analysis with LC-MS/MS. The microdialysis probes in the striata were perfused with Ringer solution at a flow of 2  $\mu$ L.min<sup>-1</sup> (CMA/102 Microdialysis Pump, Sweden). The analysis of the microdialysate samples are described below.

## 2.8 Analytical method

### 2.8.1 *in vitro* samples

Different HPLC methods were developed, in order to analyze simultaneously the respective prodrug, the parent drug 5-OH-DPAT and, if required, acetaminophen by RP-HPLC using a Superspher<sup>®</sup> 60 RP-select B, 75 mm-4 mm column (Merck KGaA, Darmstadt, Germany). The prodrugs of 5-OH-DPAT and acetaminophen were detected using a UV detector (Dual  $\lambda$  Absorbance Detector 2487, Waters, Milford, USA). The absorption wavelengths for the prodrugs and acetaminophen were 220 nm and 243 nm respectively. 5-OH-DPAT was detected using a scanning fluorescence detector (Waters<sup>™</sup> 474, Millipore, Milford, MA, USA) with excitation wavelength and emission wavelength of 276 nm and 302 nm, respectively. The composition of the mobile phase for analyzing the respective prodrug together with 5-OH-DPAT is presented in Table 1. The flow rate was set to 1.5 ml.min<sup>-1</sup> and the

volume of injection was 200  $\mu\text{l}$ . Calibration curves showed a linear response when using concentrations of compounds between 0.1 and 40  $\mu\text{g}\cdot\text{ml}^{-1}$  ( $R^2 > 0.999$ ). The limit of detection (LOD) and limit of quantification (LOQ) for these HPLC methods can also be found in Table 1.

### 2.8.2 Blood samples of (S)-5-OH-DPAT

Since the hydrolysis of  $\beta$ -ala-(S)-5-OH-DPAT to (S)-5-OH-DPAT is occurring very rapidly in human blood plasma ( $t_{1/2} = 0.24$  min in 80% human blood plasma), only (S)-5-OH-DPAT was analyzed in plasma [10]. Blood samples of 5-OH-DPAT were analyzed with an on-line solid-phase-extraction-liquid-chromatography-mass spectrometry/mass spectrometry (SPE-LC-MS/MS) method, described elsewhere [1]. Briefly, after addition of the internal standard ( $d_2$ -5-OH-DPAT; 5  $\text{ng}\cdot\text{ml}^{-1}$ ) to the collected plasma, acetonitrile was added to precipitate the proteins. The mixture was vortexed, centrifuged, after which the supernatant was dried and redissolved in MilliQ and injected on the SPE cartridge (Hysphere Resin C8, endcapped, 10 x 4 mm (ID), 10 $\mu\text{m}$  SPE cartridge (Spark Holland B.V, The Netherlands). An external

**Table 1:** Physicochemical properties of the different molecules investigated (Mw, charge/Mw ratio and cLogP) and the composition of the mobile phase with the corresponding limit of detection (LOD) and limit of quantification (LOQ)

Compound	Mw ( $\text{g}\cdot\text{mol}^{-1}$ )	Charge/ Mw ( $\times 10^3$ ) ( $\text{mol}\cdot\text{g}^{-1}$ )	clogP <sup>a</sup>	Mobile phase		LOD ( $\mu\text{g}\cdot\text{ml}^{-1}$ )	LOQ ( $\mu\text{g}\cdot\text{ml}^{-1}$ )
				Composition (v/v)	TEA (mM)		
gly-5-OH-DPAT	304.4	6.6	3.6	Ace 50 mM/ACN 85/15	0	n.d	n.d
pro-5-OH-DPAT	344.5	5.8	4.1	Ace 50 mM /ACN 74/26	0	n.d	n.d
val-5-OH-DPAT	346.5	5.8	4.8	Ace 100 mM /THF 95/5	30	0.25	0.41
$\beta$ -ala-5-OHDPAT	318.4	6.3	3.8	Ace 100 mM/THF 97.5/2.5	30	1.6	2.7
5-OH-DPAT	247.4	4.0	4.3	*		$1.4 \cdot 10^{-3}$	$2.4 \cdot 10^{-3}$
acetaminophen	151.2	0.0	n.d	*		$0.9 \cdot 10^{-3}$	$1.4 \cdot 10^{-3}$

Ace: acetatebuffer pH 3.6; nd: not determined; \* :mobile phase is dependent on the prodrug investigated  
<sup>a</sup>cLogP was calculated using ACD/Chemsketch [15-17]; n.d.: not determined

binary HPLC pump (Gynkotek, Germany) and an external Agilent 1200, 2/6 switch valve (Agilent Technology, USA) were used for the SPE sample trapping. First the SPE cartridge was conditioned, then the injected sample was trapped, consequently the valve was switched placing the SPE cartridge in-line with the LC system for elution on to the analytical column, after which the SPE cartridge was cleaned. Finally the cartridge was conditioned again. To analyze the extracted sample an Agilent 1200 HPLC system with autosampler (Agilent Technology, USA) was coupled online with an Agilent 6460 Triple Quadrupole mass spectrometer (Agilent Technology, USA). The samples were analyzed by  $\mu$ PLC-MS/MS using an Altima HP C18 column (150X 1.0 mm; 5  $\mu$ m) (Grace Davison Discovery Sciences, Belgium). The detection was performed with a triple quadrupole mass spectrometer in the positive-ion electrospray mode and all analytes were monitored with Multiple Reaction Monitoring (MRM). System operation and handling the acquired data was performed using Agilent MassHunter data acquisition software (version, B.02.00; Agilent). Calibration curves showed a linear response when using concentrations of compounds between 0.2 and 50 ng.ml<sup>-1</sup> ( $r^2 > 0.999$ ). The recovery, limit of detection (LOD) and limit of quantification (LOQ) were experimentally determined at  $93.9 \pm 2.9 \%$ , 0.07 and 0.2 ng.ml<sup>-1</sup>, respectively.

### 2.8.3 Microdialysate samples

To analyze the striatal 5-OH-DPAT concentration the dialysate from the probe in the left striatum was collected every 15 min resulting a total volume of 30  $\mu$ L per sample. The solution was analyzed using LC-MS/MS method, described elsewhere [1]. Briefly, *d*<sub>2</sub>-5-OH-DPAT.HBr was added as internal standard to a 100  $\mu$ L mixture of water + 0.1% formic acid and Ringer (1:1). The HPLC system consisted of a Shimadzu LC 20 AD binary system with a Shimadzu SIL 20AC autosampler. The samples were injected on a Grace Alltech Alltima HP C18 EPS reverse-phased column (150 x 2.1 mm (ID), 3  $\mu$ m). The compounds were detected on a SCIEX API3000 triple quadrupole mass spectrometer (Applied Biosystems/MDS SCIEX) equipped with a Turbo Ion Spray interface. The mass spectrometer was operated in the positive ion mode with MRM. The detection limit of 5-OH-DPAT was 12.5 pg.ml<sup>-1</sup>.

The dialysate contents of dopamine (DA) and its metabolites were quantified from the probe implanted at the right striatum by an on-line HPLC with electrochemical detection with the detection limit of 1 fMol per sample. An HPLC pump (LC-10AD vp, Shimadzu, Japan) was used in conjunction with an analytical cell (5011A, ESA, Chelmsford, MA, USA) and an electrochemical detector (Coulochem II, ESA)

working at +300 mV for DOPAC and HIAA and -300 mV for DA. The analytical column was a Supelco Supelcosil™ LC-18-DB column (150 mm x 4.6 mm (I.D.), 3µm). Data were converted into percentage of basal levels. The basal levels were determined from four consecutive samples (less than 20% variation), and set at 100%. After the experiments the rats were sacrificed and the brains were removed. After removal, the brains were kept in 4% paraformaldehyde solution until they were sectioned to control the location of the dialysis probes.

## 2.9 Data modeling

The data of the *in vitro* transport of valine-, β-alanine-5-OH-DPAT and 5-OH-DPAT and the PK-PD data following transdermal iontophoresis of β-alanine-(S)-5-OH-DPAT were analyzed using non-linear mixed effects modeling.

### *in vitro* model

Previous studies suggested that two transport routes are involved in the iontophoretic delivery, linked in parallel [18]. Therefore to describe the iontophoretic transport across the skin, one zero order mass input  $I_0$  from donor compartment into the skin during current application and two first order release constants  $K_{R1}$  and  $K_{R2}$  from skin to acceptor are used (Figure 2). The iontophoretic flux *in vitro* during iontophoresis can be described with the following equations:

$$J(t) = \frac{I_0}{S} (1 - e^{-K_{R1} \cdot (t-t_L)}) + \frac{I_0}{S} (1 - e^{-K_{R2} \cdot (t-t_L)}) \quad (1)$$

$$J_{ss} = 2 \cdot \frac{I_0}{S} \quad (2)$$

where  $J(t)$  is the flux at time  $t$  and  $S$  is the diffusion area and  $t_L$  is the kinetic lag time parameter, introduced to address the time required for drug molecules to enter the skin compartment and  $J_{ss}$  as the flux at steady state.

During the post iontophoresis period only one release constant is sufficient to describe the passive flux, resulting in the following equation:

$$J(t) = \frac{P_{PI}}{S} (1 - e^{-K_{R2} \cdot (t-T)}) + \left( \frac{I_0}{S} (1 - e^{-K_{R1} \cdot (T-t_L)}) + \frac{I_0}{S} (1 - e^{-K_{R2} \cdot (T-t_L)}) \right) \cdot e^{-K_{R2} \cdot (t-T)} \quad (3)$$

where  $T$  is time of current application and  $P_{PI}$  is the zero order drug input due to the passive driving force in the post iontophoretic period.



iontophoresis [19]. It is believed that during transport of the prodrug into and through the skin 2 effects occur: hydrolysis and depot formation. The resulting effect of both mechanisms is described with the addition of an extra compartment, as illustrated in Figure 2. The differential equations to describe the plasma concentration of (S)-5-OH-DPAT following transdermal iontophoretic delivery of  $\beta$ -ala-(S)-5-OH-DPAT are:

$$\frac{dX_1(t)}{dt} = I_0 \cdot N - K_R \cdot X_1(t) - k_{14} \cdot X_1(t) \quad (4)$$

$$\frac{dX_2(t)}{dt} = K_R \cdot X_1(t) + k_{32} \cdot X_3(t) + k_{42} \cdot X_4(t) - k_{23} \cdot X_2(t) - k \cdot X_2(t) \quad (5)$$

$$\frac{dX_3(t)}{dt} = k_{23} \cdot X_2(t) - k_{32} \cdot X_3(t) \quad (6)$$

$$\frac{dX_4(t)}{dt} = k_{14} \cdot X_1(t) - k_{42} \cdot X_4(t) \quad (7)$$

With  $\frac{dX_i(t)}{dt}$  as the rate of change in the amount of the drug in compartment  $i$ ,  $X_i$  as the amount of the drug in compartment  $i$ , which refers to the skin compartment ( $i=1$ ), the plasma compartment ( $i=2$ ), the peripheral compartment ( $i=3$ ) and the hydrolysis compartment ( $i=4$ ).  $I_0$  is defined as the zero order mass input,  $K_R$  as the first order release rate constant from skin to plasma,  $k$  as the first order elimination rate constant,  $k_{23}$  and  $k_{32}$  as the first order distribution rate constants from plasma to tissue and tissue to plasma, respectively.  $k_{14}$  and  $k_{42}$  are the rate constants for the mass transfer from the skin to hydrolysis compartment and from the hydrolysis compartment to the systemic circulation.  $N$  is a flag in the model to indicate that the input rate  $I_0$  is only valid during the iontophoresis period.

### PD model

An effect compartment model was used to describe the dopamine release following transdermal iontophoresis of  $\beta$ -ala-(S)-5-OH-DPAT. The rate of change of drug concentration  $\frac{dC_e(t)}{dt}$  in the effect compartment can be described as follows:

$$\frac{dC_e(t)}{dt} = k_{eo} \cdot (C_2(t) - C_e(t)) \quad (8)$$

With  $k_{e0}$  as the rate constant from plasma to the effect compartment and the elimination rate constant from the effect compartment. The striatal dopamine release  $C_{DA}$ , which is the pharmacodynamic end-point, is described by the sigmoid  $I_{max}$  model using the following equation:

$$C_{DA} = C_{DA}(0) \cdot \left( 1 - \frac{I_{max} \cdot C_e(t)^H}{IC_{50}^H + C_e(t)^H} \right) \quad (9)$$

Where  $I_{max}$  is the maximum inhibition of the dopamine production,  $IC_{50}$  is the plasma concentration of 5-OH-DPAT to produce 50% of  $I_{max}$ ,  $H$  is the Hill-slope coefficient,  $C_{DA}(0)$  is the baseline values of dopamine (i.e., dopamine concentration prior to the inhibiting effect of 5-OH-DPAT).

PK-PD data following IV infusion and transdermal delivery of (S)-5-OH-DPAT, obtained from literature, were included in the data set to obtain more reliable parameter estimates [1]. In analogy to the PK-PD model of (S)-5-OH-DPAT a covariate of route of administration for  $IC_{50}$  was added [1]. The fixed effect parameters ( $\theta$ ) included:  $I_0$ ,  $K_R$ , clearance ( $CL$ ), inter compartmental clearance ( $Q$ ), volume of the central compartment ( $V_2$ ), volume of the peripheral compartment ( $V_3$ ),  $k_{e0}$ ,  $I_{max}$ , and  $IC_{50}$ . Variability in pharmacokinetic parameters was assumed to be log-normally distributed in the population. Inter-individual variability was modeled by an exponential error model as written in Equation 10:

$$P_i = \theta \cdot \exp(\eta_i) \quad (10)$$

in which  $\theta$  is the population value for the fixed effect parameter  $P$ ,  $P_i$  is the individual estimate and  $\eta_i$  is the normally distributed interindividual random variable with mean zero and variance  $\omega^2$ . The coefficient of variation (CV %) of the structural model parameters is expressed as percentage of the root mean square of the interindividual variability term. The residual error was modeled by a proportional error model as written in Equation 11:

$$C_{obs,ij} = C_{pred,ij} \cdot (1 + \varepsilon_{ij,1}) + \varepsilon_{ij,2} \quad (11)$$

where  $C_{obs,ij}$  is the  $j$ th observed concentration in the  $i$ th individual,  $C_{pred,ij}$  is the predicted concentration, and  $\varepsilon_{ij}$  is the normally distributed residual random variable with mean zero and variance  $\sigma^2$ . The estimation of the final population parameters was performed using the conventional first order estimation method (FOCE). The PK model parameters were estimated independently and subsequently used as input for

the PD analysis. During model building, goodness-of-fit was based on statistical and graphical diagnostic criteria. Model selection and identification was based on the likelihood ratio test, coefficient of variation of parameter estimates, parameter correlations and goodness-of-fit plots. For the likelihood ratio test, the significance level for the inclusion of one parameter was set at  $p < 0.05$ , which corresponds with a decrease of 3.84 points, in the minimum value of the objective function (MVOF) under the assumption that the difference in MVOF between two nested models is  $\chi^2$  distributed. The following goodness-of-fit plots were subjected to visual inspection to detect systemic deviations from the model fits: individual observed versus population and individual predicted values. Finally, the performance of the population PK and PK-PD models were assessed by simulating 100 data sets with the final model parameter estimates. The evaluation of model performance also included visual predictive check (VPC), as implemented in Xpose 4 (R version 2.7.0, R-foundation) [20].

## 2.10 Data analysis

All data are presented as mean  $\pm$  standard deviation (SD). When a statistical analysis was performed comparing only 2 groups, a Students t-test was used. When 3 or more groups were compared, a 1-way ANOVA statistical analysis was executed. Comparing effect of two factors simultaneously was performed using 2-way ANOVA. If the overall p-value was less than 0.05, a bonferonni post-test was applied to compare different groups. For all statistical analysis a significance level of  $p < 0.05$  was used.

## 3 Results

### 3.1 Stability of prodrugs of 5-OH-DPAT in different conditions

A series of prodrugs of 5-OH-DPAT were synthesized by esterification of 5-OH-DPAT with different amino acids [10]. Because ester bounds are known to be susceptible to hydrolysis, the chemical stability of prodrugs was investigated. The various conditions were selected to mimic the conditions in the different compartments during iontophoretic transport. Apparent first order rate constants for hydrolysis were determined from the slopes of various plots of percent remaining prodrug vs time. The corresponding half lives are presented in Figure 3. Glycine-5-OH-DPAT and proline-5-OH-DPAT show a limited chemical stability in a citric buffer pH 5.0 at room temperature with a half life of 9.6 and 7.5 h, respectively. Valine-5-OH-DPAT and  $\beta$ -alanine-5-OH-DPAT are stable under this condition with

a half life of 318 and 692h, respectively. However increasing the pH from 5.0 to 6.2 at room temperature (RT) decreases the half life of both valine- and  $\beta$ -alanine-5-OH-DPAT to 7.6 h and to 64.2h, respectively. Further increasing the pH to 7.4 decreases the half life of the prodrugs to 0.7 and 4.5h for valine- and  $\beta$ -alanine-5-OH-DPAT, respectively. Increasing the temperature from RT to 32 °C, the skin temperature, decreased the stability of glycine-, valine- and  $\beta$ -alanine-5-OH-DPAT. For instance the half life of valine-5-OH-DPAT at pH 6.2 decreases from 7.6 to 5.1h when increasing the temperature. Current application and the presence of HSC however do not affect the stability of the prodrugs. Since valine- and  $\beta$ -alanine-5-OH-DPAT are the most stable prodrugs, these 2 compounds were selected for further investigations, concerning solubility and transdermal transport.

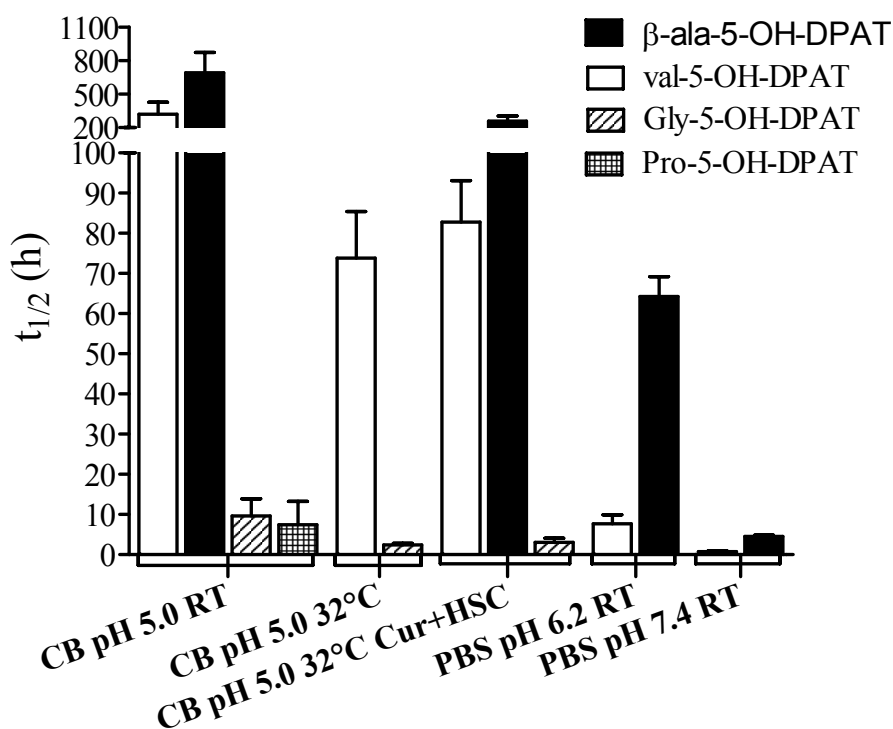


**Figure 3:** The half life ( $t_{1/2}$ ) of the hydrolysis of the prodrugs glycine-5-OH-DPAT (striped bar), proline-5-OH-DPAT (blocked bar), valine-5-OH-DPAT (white bar) and  $\beta$ -alanine-5-OH-DPAT (black bar) under various conditions. The data are presented as estimate + the upper limit of the estimate. CB: citric buffer 5 mM; RT: room temperature; HSC: human stratum corneum; Cur: current 320  $\mu$ A.

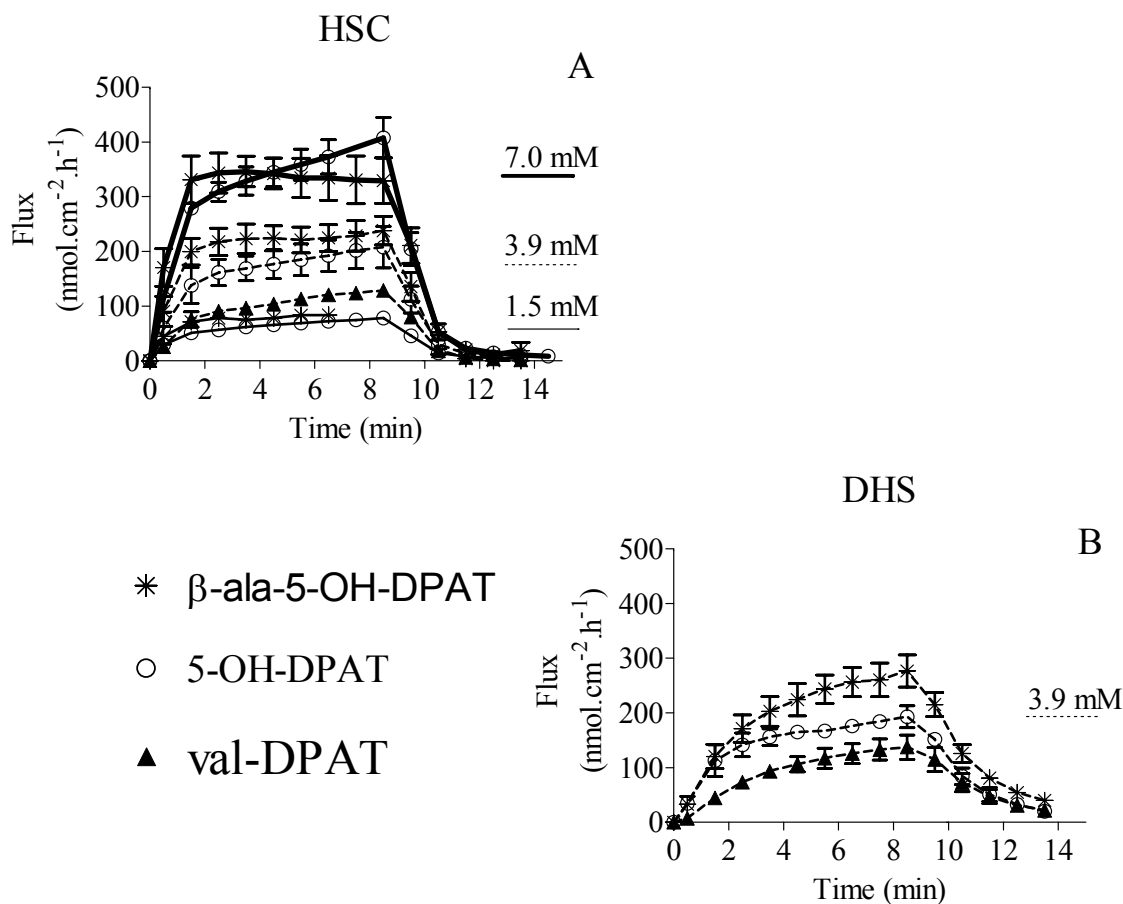


**Figure 4:** *In vitro* flux profiles of valine-5-OH-DPAT (closed triangle),  $\beta$ -ala-5-OH-DPAT (star) and 5-OH-DPAT (open circle). **A:** Iontophoresis of valine-5-OH-DPAT (only 3.9 mM (intermittent line)) and  $\beta$ -ala-5-OH-DPAT and 5-OH-DPAT at 3 different concentrations (1.5 (solid line), 3.9 (intermittent line), 7.0 mM (thick solid line)) across stratum corneum. **B:** Iontophoresis of 3.9 mM valine-5-OH-DPAT,  $\beta$ -ala-5-OH-DPAT and 5-OH-DPAT across dermatomed human skin. PBS pH 7.4 was used in all experiments as acceptor phase.

### 3.2 Solubility of valine- and $\beta$ -alanine-5-OH-DPAT

The maximum solubility was determined in citric buffer 5 mM pH 5.0 as this is the donor solution, used for transport studies. The maximum solubility of valine-5-OH-DPAT is 232.2 mM. With respect to  $\beta$ -alanine-5-OH-DPAT the maximum solubility

is expected to be higher than 832.2 mM. At this concentration the maximum solubility of  $\beta$ -alanine-5-OH-DPAT is not yet reached. However, the study was discontinued due to the limited availability of the compound.

### 3.3 *In vitro* iontophoresis of the two prodrugs in comparison to 5-OH-DPAT

Figure 4 illustrates the iontophoretic flux profiles of the prodrugs at different concentrations under various conditions. The flux profiles of the parent drug, adapted from literature, were added to the graphs for comparison [21]. In case of the prodrugs the non-hydrolyzed and the hydrolyzed fraction of the prodrug are added and the resulting total flux is displayed in Figure 4. The iontophoretic transport across HSC of the two prodrugs was evaluated in comparison to each other and their parent drug 5-OH-DPAT, using PBS pH 7.4 as acceptor phase (Figure 4A). The flux after 9h current application of  $\beta$ -alanine-5-OH-DPAT ( $238.0 \pm 26.1$  and  $329.6 \pm 41.9$   $\text{nmol.cm}^{-2}.\text{h}^{-1}$ ) across HSC is not significantly different from the flux of the parent drug 5-OH-DPAT ( $207.7 \pm 38.0$  and  $407.7 \pm 37.0$   $\text{nmol.cm}^{-2}.\text{h}^{-1}$ ) at 3.9 and 7.0 mM donor concentrations ( $p > 0.05$ ; 2-way ANOVA). Since the assay of iontophoretic delivery of 1.5 mM  $\beta$ -alanine-5-OH-DPAT was stopped after 7h of current application this time point was chosen to compare the flux of prodrug and parent drug. A similar flux was observed for  $\beta$ -alanine-5-OH-DPAT ( $84.1 \pm 5.6$   $\text{nmol.cm}^{-2}.\text{h}^{-1}$ ), compared to 1.5 mM 5-OH-DPAT ( $78.2 \pm 6.2$   $\text{nmol.cm}^{-2}.\text{h}^{-1}$ ) ( $p < 0.05$ ; t-test).

The results of the transport studies across DHS, with PBS pH 7.4 as acceptor phase, are depicted in Figure 4B. 2-way ANOVA was performed to analyze the Flux after 9h of current application ( $\text{Flux}_{9\text{h}}$ ) across HSC and DHS for all the compounds at 3.9 mM. An overall significant difference could be observed between the  $\text{Flux}_{9\text{h}}$  of the different compounds, which was due to compound variation and not due to the use of the different skin types ( $p < 0.05$ ). Bonferonni's post-test demonstrated that the  $\text{Flux}_{9\text{h}}$  of the prodrug  $\beta$ -alanine-5-OH-DPAT is significantly higher compared to the  $\text{Flux}_{9\text{h}}$  of valine-5-OH-DPAT across DHS and HSC. In addition only across DHS the  $\text{Flux}_{9\text{h}}$  of  $\beta$ -alanine-5-OH-DPAT is significantly higher than the  $\text{Flux}_{9\text{h}}$  of the parent drug, 5-OH-DPAT. Furthermore the  $\text{Flux}_{9\text{h}}$  of valine-5-OH-DPAT was significantly lower compared to the  $\text{Flux}_{9\text{h}}$  of the parent drug across HSC and DHS.

Acetaminophen (15 mM) as electroosmotic marker was added to the donor concentration to quantify the electroosmotic flux. 1-way ANOVA, with a bonferonni post test showed that the electroosmotic flux during transport of valine-5-OH-DPAT ( $7.8 \pm 1.9$   $\text{nmol.cm}^{-2}.\text{h}^{-1}$ ) is significantly lower than the electroosmotic flux of 5-OH-DPAT ( $13.7 \pm 3.4$   $\text{nmol.cm}^{-2}.\text{h}^{-1}$ ) ( $p < 0.05$ ), however not significantly different from

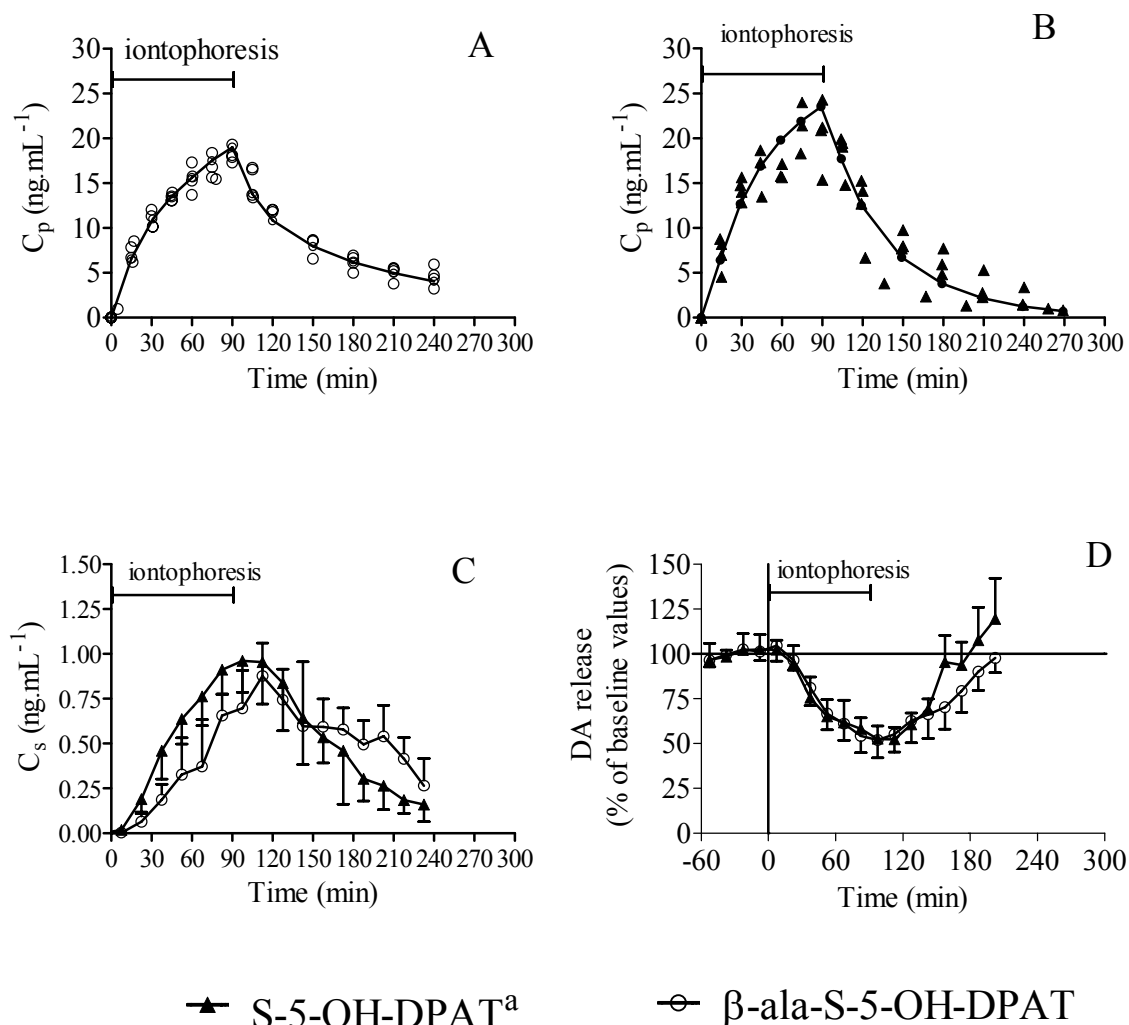


**Figure 5:** Resulting graphs of the PK-PD study with  $\beta$ -ala-(S)-5-OH-DPAT (open circle) together the results of (S)-5-OH-DPAT (closed triangle), adapted from literature. The observed plasma concentration ( $C_p$ ) of (S)-5-OH-DPAT, following transdermal iontophoresis of  $\beta$ -ala-(S)-5-OH-DPAT (A) and (S)-5-OH-DPAT (B) are presented together with the population prediction (PRED) (full line).

C: The striatal concentration of (S)-5-OH-DPAT ( $C_s$ ), presented as mean  $\pm$  SD, following iontophoretic delivery of  $\beta$ -ala-(S)-5-OH-DPAT and (S)-5-OH-DPAT.

D: The dopamine (DA) release in the striatum, as % baseline, presented as mean  $\pm$  SD, following iontophoretic delivery of  $\beta$ -ala-(S)-5-OH-DPAT and (S)-5-OH-DPAT.

<sup>a</sup>adapted from literature [1]

$\beta$ -alanine-5-OH-DPAT ( $11.7 \pm 4.2 \text{ nmol.cm}^{-2}.\text{h}^{-1}$ ) ( $p > 0.05$ ). Also the electroosmotic flux of 5-OH-DPAT and  $\beta$ -alanine-5-OH-DPAT are not significantly different ( $p > 0.05$ ).

The iontophoretic transport profile across HSC and DHS of 3.9 mM  $\beta$ -alanine-5-OH-DPAT was modeled using Equations 1 and 3. The resulting parameters are displayed in Table 2. The estimated steady state flux, calculated with Equation 2, is higher for DHS, compared to HSC. The lag time ( $T_{lag}$ ) and passive driving force post iontophoresis ( $P_{PI}/S$ ) are also higher for DHS, whereas the release constants  $K_{R1}$  and  $K_{R2}$  are lower compared to HSC.

### 3.4 Hydrolysis during transport through HSC and DHS

Approximately  $19.8 \pm 2.6\%$  and  $55.4 \pm 15.1\%$  of  $\beta$ -alanine-5-OH-DPAT is hydrolyzed in 5-OH-DPAT when transported across HSC and DHS, respectively, using PBS pH 7.4 as acceptor phase. A similar observation is found for val-5-OH-DPAT, using PBS pH 6.2 as acceptor phase:  $26.8 \pm 5.4\%$  and 100% valine-5-OH-DPAT is converted into 5-OH-DPAT when transported through HSC and DHS, respectively.

### 3.5 *In vivo* iontophoretic delivery of $\beta$ -ala-(S)-5-OH-DPAT

The PK and PD of the active S-enantiomer of the most promising prodrug  $\beta$ -ala-(S)-5-OH-DPAT following transdermal delivery were investigated simultaneously. For comparison the plasma-, striatum profile and the dopamine release following transdermal iontophoresis of the parent drug (S)-5-OH-DPAT, adapted from literature, are added to the resulting graphs (Figure 5B-D) [1].

#### 3.5.1 Plasma profile

The prodrug is rapidly hydrolyzed to (S)-5-OH-DPAT in blood plasma, since the half life is 0.24 min in 80% human blood plasma [10]. Therefore the plasma concentration of the parent drug (S)-5-OH-DPAT was monitored during the PK-PD study. No detectible amount of (S)-5-OH-DPAT was observed after 15 min of passive diffusion (data not shown). Current application starts at  $t=0$  min, as depicted in Figure 5A. As can be observed current application results in immediate increase in plasma concentration. After 90 min of current application, the plasma profile tends towards a steady state situation. The resulting plasma concentration at time=90 min is  $18.2 \pm 0.8 \text{ ng.ml}^{-1}$ . After current application is discontinued and the patch is removed, the profile shows a decline in plasma concentration, which is best described with a 2-compartmental model.

**Table 2:** The resulting population estimates of simultaneous modeling the plasma concentration and dopamine release following transdermal iontophoresis of  $\beta$ -ala-(S)-5-OH-DPAT (3.9 mM) in male wistar rats. The resulting parameters of fitting the *in vitro* transdermal iontophoretic transport of  $\beta$ -ala-5-OH-DPAT (3.9 mM) across human stratum corneum (HSC) and dermatomed human skin (DHS) is depicted. PBS pH 7.4 was used as acceptor phase for the *in vitro* experiments

parameter	unit	Between animal variability				Between subject variability					
		Estimate	RSE %	Estimate	RSE %	Estimate	RSE %	Estimate	RSE %		
<b>PK-PD</b>											
$V_2$	L	0.46	18	0.13	97	<b>HSC (<i>in vitro</i>)</b>					
$V_3$	L	0.78	16	0.07	52	$J_{ss}$ 500	*	272.5	4		
CL	L.h <sup>-1</sup>	2	6	0.02	38	$K_{R1}$	h <sup>-1</sup>	0.278	28	0.516	82
Q	L.h <sup>-1</sup>	1.96	21	0.16	73	$K_{R2}$	h <sup>-1</sup>	1.69	8	0.035	23
$J_{ss}$ 250	*	110.6	8			$T_{lag}$	h	0.005			
$K_R$	h <sup>-1</sup>	0.31	23			Pass	*	n.d.			
$k_{14}$	h <sup>-1</sup>	5.06	23			Sigma 1		0.019	17		
$k_{42}$	h <sup>-1</sup>	4.79	21			Sigma 2		1.93	36		
$k_{eo}$	h <sup>-1</sup>	3.79	12	0.19	48	<b>DHS (<i>in vitro</i>)</b>					
IC <sub>50</sub>	ng.ml <sup>-1</sup>	4.50	12	0.07	35	$J_{ss}$ 500	*	381.3	7		
N		3.12	9			$K_{R1}$	h <sup>-1</sup>	0.069	35	0.212	23
$I_{max}$		40.9	7	0.03	39	$K_{R2}$	h <sup>-1</sup>	0.588	5	0.3	51
						$T_{lag}$	h	0.22	10		
						Pass	*	29.1	14	0.045	33
Sigma 1	PK	0.02	24			Sigma 1		0.002	67		
Sigma 1	PD	0.01	20			Sigma 2		18.4	59		

\*: unit of  $J_{ss}$  and Pass is: nmol.cm<sup>-2</sup>.h<sup>-1</sup>

Sigma 1: proportional error; Sigma 2: additive error

n.d.: not determined because the parameter value was constrained to 0

### 3.5.2 Striatum profile

The 5-OH-DPAT concentration of the microdialysate samples of the left striatum was analyzed following transdermal iontophoresis of  $\beta$ -ala-(S)-5-OH-DPAT. With a delay of approximately 7.5 min, the striatal 5-OH-DPAT concentration ( $C_s$ ) increased when starting iontophoresis to a maximum level of  $0.88 \pm 0.18 \text{ ng.ml}^{-1}$ . This maximum was reached 22.5 min after switching off the current ( $t=112.5 \text{ min}$ ). After this time point  $C_s$  declines again.

### 3.5.3 Pharmacodynamic effect

With on-line microdialysis the DA concentration (the pharmacodynamic end-point) in the right striatum was monitored. The resulting DA release profile (mean  $\pm$  SD) is depicted in Figure 5D. Prior to iontophoresis the DA level was monitored and the average DA level from 4 consecutive points was set to 100%. As can be observed, when starting iontophoresis the DA level decreases with a lag time between 7.5 and 22.5 min. The DA level decreases to near steady state level of  $48.6 \pm 8.2\%$  baseline, 94.5 min after the start of iontophoresis. After removal of the patch, the DA level recovers again to its initial state (DA release=100%) at time= $189.2 \pm 12.1 \text{ min}$  following prodrug iontophoresis.

## 3.6 Non-linear mixed effects modeling: model evaluation

The *in vitro* transport flux profiles, the plasma profile and the pharmacodynamic effect are modeled with non linear mixed effects modeling, using compartmental models. The resulting parameter estimates are depicted in Table 2. A relatively low Residual Standard Error (RSE%) for the fixed *in vitro* ( $\leq 35\%$ ) and *in vivo* parameters estimates ( $\leq 23\%$ ) indicates a reliable prediction of the estimates. Moreover Figure 6A and B, displaying the visual predictive check (VPC), demonstrates that the *in vivo* observations are well distributed between the 2.5<sup>th</sup> and the 97.5<sup>th</sup> percentiles. This indicates that the variability, predicted by the PK-PD model, corresponds with the observed variability. In addition the diagnostic plots of the PK and PD profile, shown in Figure 6C-F, indicate that the proposed PK-PD model adequately describes the plasma profile and pharmacodynamic effect.

## 4 Discussion

The general aim of the present study is to evaluate different prodrugs and select the best candidate(s) for transdermal iontophoretic delivery. The presence of enzymes in the skin, such as esterases and amidases, makes the use of prodrugs an interesting

approach for transdermal delivery. The prodrugs can be tailored to improve drug delivery and during transport across the skin, the enzymes hydrolyze the prodrugs to their active parent drug [8].

#### 4.1 Chemical stability and solubility

Ester prodrugs, as presented in this paper, are not only susceptible to enzymatic, but also to chemical hydrolysis. The stability of the prodrugs in different aqueous solutions is highly dependent on the side chain, esterified with 5-OH-DPAT (stability: glycine < proline < valine <  $\beta$ -alanine). Based on these results valine- and  $\beta$ -alanine-5-OH-DPAT were selected for further investigating the transdermal iontophoretic transport across human skin. Esterification of 5-OH-DPAT with valine and  $\beta$ -alanine improved its solubility tremendously. The solubility of valine- and  $\beta$ -alanine-5-OH-DPAT was respectively 4 and more than 14 times higher, compared to its parent drug 5-OH-DPAT [21]. A higher solubility enables reduction of the patch volume, while keeping sufficient amount of drug in the patch. Presumably addition of an extra chargeable amine group contributes substantially to the solubility of the prodrugs.

#### 4.2 Transdermal iontophoresis *in vitro*

At pH 5.0 both prodrugs have an additional charge compared to 5-OH-DPAT. When increasing the charge from monovalent to bivalent, this affects in several ways the transport: (i) bivalent ions have a larger hydrated volume, as suggested by Lai and Roberts, which can result in a reduced flux [22], (ii) bivalent ions interact more with charged sites in SC, which according to Phipps *et al.* will result in a reduced flux [23] and (iii) an increase in the charge/molecular weight ratio results in an equivalent higher electromigrative flux [24]. It is suggested that the lipophilicity, indicated by the cLogP (Table 1), of the prodrugs influences the balance between these three factors and therefore affects the transport efficiency [15-17]. Only for the more hydrophilic prodrug  $\beta$ -alanine-5-OH-DPAT with a charge/Mw ratio which is 1.5 times higher compared to 5-OH-DPAT, resulted in almost in an equivalent increase (1.4 times) in the total flux after 9h of current application across DHS. The flux of  $\beta$ -alanine-5-OH-DPAT is less affected by the increased hydrated volume and the skin interaction. In contrast valine-5-OH-DPAT with a hydrophobic prodrug moiety is retained more by the skin and shows a decreased flux compared to 5-OH-DPAT. This hypothesis is strengthened by the decreased electroosmotic flux during transport of valine-5-OH-DPAT. Valine-5-OH-DPAT is retained more strongly and the two positive charges cause a neutralization of the skin negative charges, resulting in a

**VPC PK - PD**

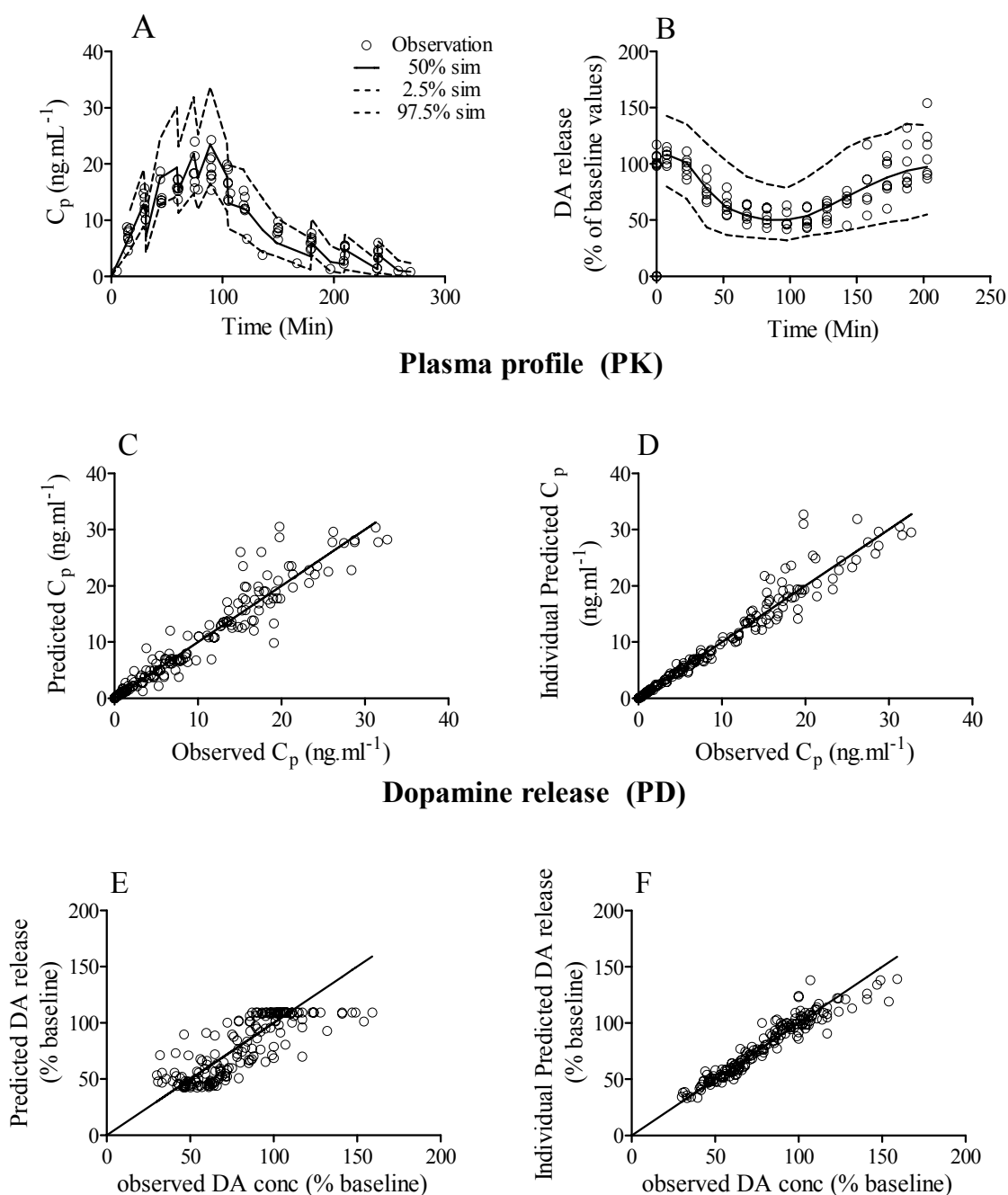


**Figure 6:** Diagnostic plots of simultaneous fitting the plasma concentration (A, C, D) and the dopamine release (B, E, F) following the transdermal iontophoresis of  $\beta$ -ala-(S)-5-OH-DPAT. Depicted are the observations (open circles) together with the interquartile concentration range (2.5%-97.5%, intermittent line) and the median (50%, solid line) of the plasma profile (A) and the dopamine release profile (B). A number of 100 samples were simulated based on the final parameter estimates. C,E: population predicted vs the observed data. D,F: individual prediction vs the observed data.

reduced electroosmotic flux. Furthermore, the transport of valine-5-OH-DPAT is less affected by the charge/molecular weight ratio. These results are in agreement with the computational studies performed by Schuetz *et al.*, who predicted with a 3D quantitative structure-permeation relationship that iontophoresis was favored by peptide hydrophilicity and hindered by voluminous localized hydrophobicity [25].

Besides the transport efficiency it is also important to determine the rate of hydrolysis during iontophoretic transport across human skin in order to be able to predict the amount of prodrug and parent drug that will be taken up by the blood stream. In analogy to the chemical stability,  $\beta$ -alanine-5-OH-DPAT is the more stable prodrug. For both prodrugs an increased hydrolysis is observed when transported across DHS. This increased hydrolysis rate is the result of 2 mechanisms. Firstly the presence of enzymes, such as esterases, is more abundant in the epidermis [13]. Secondly the increased migration time through DHS and the slower release from the DHS, reflected by  $K_{R1}$  and  $K_{R2}$  (Table 2), results in a possibly longer interaction of enzymes with the prodrugs augmenting the hydrolysis rate. The remaining prodrug that is not hydrolyzed during transdermal transport is expected to be hydrolyzed rapidly when taken up by the blood stream, since the enzymatic half life of valine- and  $\beta$ -alanine-5-OH-DPAT in 80% human blood plasma was 0.22 and 0.24 min, respectively [10].

### 4.3 PK-PD properties

The pharmacokinetic and pharmacodynamic properties of  $\beta$ -alanine-(S)-5-OH-DPAT, the more stable and soluble prodrug with improved *in vitro* transport efficiency, were investigated in an animal model. Under anesthetized conditions blood samples were taken and the dopamine level in the striatum (pharmacodynamic end-point) was monitored on-line with microdialysis. This animal model is identical to the animal model used to investigate the PK-PD properties of (S)-5-OH-DPAT, which enables us to compare the prodrug to its parent drug [1]. The plasma concentration profile of (S)-5-OH-DPAT ( $C_p$ ) following transdermal iontophoresis of the prodrug differs on 3 aspects from the profile following (S)-5-OH-DPAT administration, as can be observed in Figure 5A-B. (i) The increase in plasma concentration during current application is slower for the prodrug than for the parent drug. This is reflected by a decreased skin release constant  $K_R$  for the prodrug (Table 2) [1]. (ii) After 90 min of current application the population predicted  $C_p$  is lower for  $\beta$ -ala-(S)-5-OH-DPAT ( $19 \text{ ng}\cdot\text{ml}^{-1}$ ) than for (S)-5-OH-DPAT ( $23.5 \text{ ng}\cdot\text{ml}^{-1}$ ). (iii) During the elimination phase the  $C_p$  profile is different following administration of prodrug *vs* parent drug. It is hypothesized that these 3 differences can be partially

attributed to the hydrolysis of the prodrug during transdermal transport, assuming the hydrolysis in blood plasma is occurring instantaneously. Furthermore it is believed that after penetration through the stratum corneum depot formation of the prodrug in the viable epidermis also delays the release to the systemic circulation. The resulting effect was included in the PK-model by adding an extra compartment between the skin and the central compartment (Figure 2). This model adequately described the plasma profile following transdermal administration of the prodrug (Figure 6).

In addition the resulting parameter estimates corresponded very well with the parameters of (S)-5-OH-DPAT obtained for the PK-PD study [1]. It can be observed in Figure 5C that in analogy to  $C_p$  the increase in  $C_s$  during the absorption phase is faster and that the striatal clearance is going more rapidly following iontophoresis of the parent drug (S)-5-OH-DPAT. Finally the difference in  $C_p$  and  $C_s$  profile following prodrug vs parent drug administration resulted also in a different striatal DA release profile (Figure 5D). During the iontophoretic period no difference was observed in DA release with the same maximum. This suggests that despite a lower steady state plasma concentration the same maximum effect can be achieved. Post-iontophoresis however the time for the DA release to recover to baseline values post-iontophoresis was significantly longer for the prodrug ( $99.2 \pm 12.1$  min) compared to (S)-5-OH-DPAT ( $79.4 \pm 1.3$  min) (t-test;  $p < 0.05$ ). This can be attributed to higher  $C_p$  values after removal of the patch due to delayed skin release. On the one hand, this prolonged effect can be a drawback to initiate therapy to treat Parkinson's disease, since rapid changes in delivery schemes may be required. On the other hand, the prolonged effect of the prodrug can be beneficial for patients who suffer from nocturnal disturbances. Nocturnal disturbances are one of the most common non-motor complications in patients with Parkinson's disease [26]. It is believed that continuous stimulation of the DA receptor during the night can reduce the occurrence of nocturnal disturbances [27].

#### 4.4 *in vitro-in vivo* correlation

Fitting *in vitro* and *in vivo* transport using compartmental modeling allowed us to compare both iontophoretic transports. Different kinetic models were used to describe the *in vitro* and *in vivo* transport of the prodrug  $\beta$ -alanine-(S)-5-OH-DPAT. This suggests that different transport mechanisms can be involved *in vitro* and *in vivo*. These differences can at least partially be attributed to 3 factors. Firstly, the structure of human skin differs from the structure of rats. Mainly the thickness of the different skin layers, the stratum corneum lipid composition and the density of hair follicles will contribute to the difference [28]. But previous studies showed that

iontophoresis under constant current conditions diminishes the interspecies variations [29] and that rat skin has comparable permeation kinetic parameters with human skin [28]. Secondly the clearance of the penetrant by the acceptor flow may be different from the clearance *in vivo* by the microcirculation in the skin [28]. Thirdly, the activity of the esterase *in vivo* may be different from the esterase activity in freshly excised skin. Despite these differences a good correlation was observed between the steady state flux *in vitro* and *in vivo*. Assuming that there is a linear correlation *in vivo* between the flux and the current density [1], applying a current density of 500  $\mu\text{A}\cdot\text{cm}^{-2}$  would result in an *in vivo* steady state flux ( $J_{ss}=I_0/S$ ) of 221.2  $\text{nmol}\cdot\text{cm}^{-2}\cdot\text{h}^{-1}$ . This flux corresponded best with the *in vitro*  $J_{ss}$  across HSC (272.5  $\text{nmol}\cdot\text{cm}^{-2}\cdot\text{h}^{-1}$ ) compared to the  $J_{ss}$  across DHS (381.3  $\text{nmol}\cdot\text{cm}^{-2}\cdot\text{h}^{-1}$ ). This suggests that transport across HSC can provide valuable information for prediction towards the *in vivo* situation for this particular compound. Whether this is also the case for other drugs, remains to be established.

In conclusion this study demonstrates the potential of improving solubility, iontophoretic transport and changing the plasma profile and the PD effect of the promising dopamine agonist 5-OH-DPAT with the use of prodrugs. A good balance was found between an efficient transport rate and enzymatic conversion to the parent drug during transdermal transport. Of the synthesized prodrugs, presented in this research,  $\beta$ -alanine-5-OH-DPAT is the most promising prodrug and is a potential candidate for further investigation. This sufficiently stable prodrug shows a tremendous increase in solubility, which can be beneficial for manufacturing and practical use. The increased *in vitro* flux of  $\beta$ -alanine-5-OH-DPAT across human skin did not result in higher steady state plasma concentrations, but in a prolonged effect which reached the same maximum level as was observed with the parent drug.

## Acknowledgements

This research was financially supported by a grant (LKG 6507) of the Dutch Technology Foundation STW, Utrecht, The Netherlands. The authors thank J.B. De Vries from the Department of biomonitoring and sensing (University Center of Pharmacy, University of Groningen, the Netherlands) for his support with the animal studies.

## References

1. Ackaert, O., et al., *Controlling the pharmacokinetics and the pharmacodynamic effect of (S)-5-OH-DPAT with transdermal iontophoresis*. 2010. **submitted for publication**.
2. Coldwell, M.C., et al., *Comparison of the functional potencies of ropinirole and other dopamine receptor agonists at human D2(long), D3 and D4.4 receptors expressed in Chinese hamster ovary cells*. Br J Pharmacol, 1999. **127**(7): p. 1696-702.
3. Nugroho, A.K., et al., *Transdermal iontophoresis of rotigotine across human stratum corneum in vitro: influence of pH and NaCl concentration*. Pharm Res, 2004. **21**(5): p. 844-50.
4. van der Geest, R., M. Danhof, and H.E. Bodde, *Iontophoretic delivery of apomorphine. I: In vitro optimization and validation*. Pharm Res, 1997. **14**(12): p. 1798-803.
5. Abla, N., et al., *Topical iontophoresis of valaciclovir hydrochloride improves cutaneous aciclovir delivery*. Pharm Res, 2006. **23**(8): p. 1842-9.
6. Laneri, S., et al., *Ionized prodrugs of dehydroepiandrosterone for transdermal iontophoretic delivery*. Pharm Res, 1999. **16**(12): p. 1818-24.
7. Wang, J.J., et al., *Ester prodrugs of morphine improve transdermal drug delivery: a mechanistic study*. J Pharm Pharmacol, 2007. **59**(7): p. 917-25.
8. Guy, R.H., J. Hadgraft, and D.A. Bucks, *Transdermal drug delivery and cutaneous metabolism*. Xenobiotica, 1987. **17**(3): p. 325-43.
9. Nugroho, A.K., et al., *Pharmacokinetics and pharmacodynamics analysis of transdermal iontophoresis of 5-OH-DPAT in rats: in vitro-in vivo correlation*. J Pharm Sci, 2006. **95**(7): p. 1570-85.
10. De Graan, J., et al., *Synthesis and evaluation of the chemical and enzymatic stability of a series of novel amino acid prodrugs of the potent dopamine D2 agonist (S)-5-OH-DPAT developed for transdermal iontophoresis*. 2010. **In preparation**.
11. Westfall, T.C., et al., *The role of presynaptic receptors in the release and synthesis of 3H-dopamine by slices of rat striatum*. Naunyn Schmiedebergs Arch Pharmacol, 1976. **292**(3): p. 279-87.
12. Nugroho, A.K., et al., *Transdermal iontophoresis of the dopamine agonist 5-OH-DPAT in human skin in vitro*. J Control Release, 2005. **103**(2): p. 393-403.
13. Prusakiewicz, J.J., C. Ackermann, and R. Voorman, *Comparison of skin esterase activities from different species*. Pharm Res, 2006. **23**(7): p. 1517-24.
14. Paxinos, G. and C. Watson, *The rat brain in stereotaxic coordinates*. Academic Press: Sydney. 1982.
15. Tetko, I.V. and P. Bruneau, *Application of ALOGPS to predict 1-octanol/water distribution coefficients, logP, and logD, of AstraZeneca in-house database*. J Pharm Sci, 2004. **93**(12): p. 3103-10.
16. Tetko, I.V., et al., *Virtual computational chemistry laboratory--design and description*. J Comput Aided Mol Des, 2005. **19**(6): p. 453-63.
17. VCCLAB. *Virtual Computational Chemistry Laboratory*, <http://www.vcclab.org>. 2005.
18. Ackaert, O., et al., *Transdermal iontophoretic delivery of a novel series of dopamine agonists in vitro: physicochemical considerations* J Pharm Pharmacol, 2010. **accepted for publication**.
19. Nugroho, A.K., et al., *Compartmental modeling of transdermal iontophoretic transport II: in vivo model derivation and application*. Pharm Res, 2005. **22**(3): p. 335-46.
20. Holford, N., *The Visual Predictive Check-Superiority to Standard Diagnostic (Rorschach) Plots*. PAGE 14, Abstr 738 [[www.page-meeting.org/?abstract=738](http://www.page-meeting.org/?abstract=738)], 2005.
21. Ackaert, O.W., et al., *Mechanistic studies of the transdermal iontophoretic delivery of 5-OH-DPAT in vitro*. J Pharm Sci, 2010. **99**(1): p. 275-85.

22. Lai, P.M. and M.S. Roberts, *An analysis of solute structure-human epidermal transport relationships in epidermal iontophoresis using the ionic mobility: pore model*. J Control Release, 1999. **58**(3): p. 323-33.
23. Phipps, J.B., R.V. Padmanabhan, and G.A. Lattin, *Iontophoretic delivery of model inorganic and drug ions*. J Pharm Sci, 1989. **78**(5): p. 365-9.
24. Abla, N., et al., *Effect of charge and molecular weight on transdermal peptide delivery by iontophoresis*. Pharm Res, 2005. **22**(12): p. 2069-78.
25. Schuetz, Y.B., et al., *Structure-permeation relationships for the non-invasive transdermal delivery of cationic peptides by iontophoresis*. Eur J Pharm Sci, 2006. **29**(1): p. 53-9.
26. Comella, C.L., *Sleep disorders in Parkinson's disease: an overview*. Mov Disord, 2007. **22 Suppl 17**: p. S367-73.
27. Steiger, M., *Constant dopaminergic stimulation by transdermal delivery of dopaminergic drugs: a new treatment paradigm in Parkinson's disease*. Eur J Neurol, 2008. **15**(1): p. 6-15.
28. Godin, B. and E. Touitou, *Transdermal skin delivery: predictions for humans from in vivo, ex vivo and animal models*. Adv Drug Deliv Rev, 2007. **59**(11): p. 1152-61.
29. Kanikkannan, N., J. Singh, and P. Ramarao, *In vitro transdermal iontophoretic transport of timolol maleate: effect of age and species*. J Control Release, 2001. **71**(1): p. 99-105.



